LDV Measurements of Drop Velocity in Diesel-Type Sprays

K.-J. Wu,* D. A. Santavicca,† and F. V. Bracco‡
Princeton University, Princeton, New Jersey
and
A. Coghe§
Centro Ricerche Propulsione e Energetica CNR, Milan, Italy

Axial and radial components of the drop velocity were measured by laser Doppler velocimetry (LDV) within n-hexane-into-nitrogen sprays from single-hole cylindrical nozzles at room temperature. The gas-to-liquid density ratio, the injection velocity, and the nozzle length and diameter were varied. The LDV system included an argon-ion laser, dual beam LDV optics with frequency shifting and 90-deg collection, a counter processor, and minicomputer data acquisition. The total error in the measured mean and fluctuation drop velocities was less than 10% from the centerline to the half-radius (half-the-width at half-the-depth) and larger and more uncertain beyond it. Velocity bias was the most difficult error to quantify. It is found that beyond 300 nozzle diameters from the nozzle so much ambient gas has been entrained by the drops that the subsequent structure of the spray is dominated by the entrained ambient gas, and the fully developed incompressible jet structure and drop-gas equilibrium are being approached. This conclusion is supported by all the measured drop velocity parameters: jet half radius, centerline velocity decay, axial mean velocity distribution, axial and radial velocity fluctuation distributions, and independence of drop velocity on drop size. Large uncertainties about the magnitude of errors at the outer edges of jets using both laser Doppler velocimetry and hot-wire anemometry suggest that this region is still poorly characterized even for incompressible jets.

Nomenclature

C, C_g, C_ℓ = constants of Eqs. (1) and (2)
d = nozzle orifice diameter, μm
$F_{v,r}, F_{v,x}$ = flatness = $\overline{V_r'^4}/[\overline{V_r'^2}]^2$, $\overline{V_x'^4}/[\overline{V_x'^2}]^2$
L = nozzle passage length, μm
p_g = chamber gas pressure, MPa
r = radial coordinate, cm
$r_{0.5}$ = half-radius (half-the-width at half-the-depth) of the drop axial velocity profile, cm
$RFA_{v,x}$ = relative fluctuation amplitude (standard deviation) of the axial velocity of the drops, $=\sqrt{\overline{V_x'^2}}/V_x$
$S_{v,r}, S_{v,x}$ = skewness = $\overline{V_r'^3}/[\overline{V_r'^2}]^{3/2}$, $\overline{V_x'^3}/[\overline{V_x'^2}]^{3/2}$
U_r, U_x = radial and axial components of the gas velocity, m/s
$U_{x,\mathrm{cl}}$ = axial velocity of the gas at the centerline of the jet, m/s
V_r, V_x = radial and axial components of the drop velocity, m/s
$\bar{V}_{\mathrm{inj}}$ = mass mean injection velocity, m/s
$V_{x,\mathrm{cl}}$ = axial velocity of the liquid at the centerline of the spray, m/s
X, Y, Z = spatial coordinates (X is from the nozzle exit, see Fig. 3), cm
X_0 = virtual origin, cm
Δp = effective injection pressure, MPa
θ = gas volume fraction
μ_ℓ = liquid dynamic viscosity, kg/m·s
ρ_g = chamber gas density, kg/m^3
ρ_ℓ = liquid density, kg/m^3
σ_ℓ = liquid surface tension coefficient, kg/s^2

Superscripts

$(\bar{\ })$ = mean value
$(\ )'$ = fluctuating component

Received June 25, 1983; revision submitted Nov. 4, 1983.

*Graduate Student, Department of Mechanical and Aerospace Engineering.
†Research Engineer, Department of Mechanical and Aerospace Engineering.
‡Professor, Department of Mechanical and Aerospace Engineering.
§Research Scientist.

Introduction

THE breakup of liquid jets is achieved through a large variety of atomizers for an even larger variety of applications.[1,2] Its purpose is to increase the surface-to-volume ratio of the liquid, thus increasing the specific rates of mass, momentum, and heat transfer and the vaporization rate. Even restricting ourselves to injectors used in diesel engines, many designs exist but the most common consists of a group of cylindrical holes 100-300 μm in diameter.[3,4]

When a liquid is forced through a cylindrical hole into a gas, many modes of breakup are observed. In the one relevant in internal combustion engines, no outer intact length is seen and the jet starts diverging at the nozzle exit. All other parameters being the same, this regime, which has been called the atomization regime, is reached at high injection velocities—of the order of 100 m/s for the fuels and conditions of engine applications.[5]

Because of their practical importance, many aspects of atomizing jets have been studied extensively. In the 1930's significant data were collected on such global quantities as downstream drop sizes, tip penetration rates, and average spray angles.[1-4] More recent efforts have attempted to determine the structure of atomizing jets. For example, the outer part in the immediate vicinity of the nozzle exit[5,6] and the inner part in the same region [7] are being studied in detail. Recently, laser techniques have been used to measure drop velocity, drop size, and liquid volume concentrations at ambient pressure in gas turbine-type, dilute sprays from air blast atomizers in which more than 90% of the light is transmitted.[8]

In this paper we report drop velocity measurements within nonvaporizing, steady, diesel-type, fast, dense sprays from single-hole cylindrical nozzles into compressed nitrogen at room temperature in regions so close to the injector that light transmissivity was as low as 2%.

Conditions, Apparatus, and Procedure

n-hexane was injected into quiescent nitrogen at room temperature but at such pressures that the ratio of the gas density to the liquid density was 0.0256 and 0.0732. Three single-hole round nozzles with sharp inlet and outlet and two injection pressures (Δp 11.0 and 26.2 MPa) were used. The effect of nozzle geometry was explored by varying the diameter, 127 and 76.2 μm, and the length-to-diameter ratio, 1 and 4. These parameters, summarized in Table 1, were chosen because earlier work[5] had shown the gas-to-liquid density ratio and the nozzle geometry to be the most important variables in the initial formation of the spray and the injection velocity is important in the subsequent development and propagation of jets. Using the LDV system in the 90-deg scatter mode, it was found that reliable drop velocity measurements were possible at locations characterized by very high drop number densities ($\geq 10^{11}/m^3$) and high velocity gradients (up to 5m/s/mm). Thus, measurements were made across the jet as close as 2.3 cm from the nozzle exit.

The experimental apparatus consisted of a spray chamber, a liquid pressurization system, a nozzle assembly, and LDV optics and instrumentation. A schematic diagram of the spray chamber with the liquid pressurization system and the nozzle assembly is shown in Fig. 1 and details are available in Refs. 6 and 10.

The spray chamber was constructed from several cylindrical steel sections, 19-cm i.d. and 90 cm in total length. The window section has four quartz windows 10 cm in diameter. The liquid pressurization system was designed to maintain constant pressures up to 207 MPa during injection. The liquid pressure before injection was measured with an AMINCO 47-18340 gage and during injection with a Kistler 307A transducer with a frequency response of up to 240 kHz, a Kistler 504 charge amplifier, and a Tektronix 7313 storage oscilloscope. During data acquisition the pressure changed by less than 1%.

The single-hole round nozzles were drilled directly into the nozzle units, whic were made of AISI 303 stainless steel, and examined under a scanning electron microscope to assure that the desired inlet sharpness was obtained and not altered during the tests. Surface roughness was less than 5% of the diameter. The nozzle unit and a typical spray are shown in Fig. 2.

The liquid injection velocity was calculated from the measured injection duration, the area of the nozzle, and the total amount of liquid injected [$\bar{V}_{inj} = \text{volume}/\pi(d/2)^2\Delta t$]. This volume (mass) mean velocity was reproducible to within $\pm 1\%$. The velocity profile within the nozzle was not measured due to the nozzle's smallness and the very high velocity of the liquid, but is expected to have been flat, except near the nozzle walls, because the upstream liquid was essentially quiescent and the length-to-diameter ratio of the nozzle was much too small for transition to turbulence away from the nozzle walls. Using the measured $\bar{V}_{inj}$ and assuming ideal velocity except near the walls, we estimate the injection momentum to have been $C_\ell \rho_\ell \bar{V}_{inj}^2 \pi(d/2)^2$ with $C_\ell = 1.0 \pm 10\%$.

Two LDV systems were used. Both systems employed a Lexel 95-2 argon-ion laser operated at powers between 0.1 and 1 W and TSI dual beam focusing and 90-deg scatter collection optics. The two LDV systems used different laser wavelengths, 514.5 and 488.0 nm; fringe spacing, 6.17 and 2.45 μm; and focusing optics focal lengths, 600 and 250 mm, respectively. The second system (Fig. 3) was superior because of its capability to measure flow reversal with the TSI 9180 frequency shift unit and its smaller probe volume ($0.2 \times 0.2 \times 0.2$ mm^3 vs $0.2 \times 0.2 \times 0.7$ mm^3). When using the system with the Bragg cell the LDV signal was electronically downmixed to 0 Hz for the axial velocity component measurements in the core region where the drop velocity fluctuations were small compared to the mean velocity and to 5 MHz near the outer edge of the spray and for all the measurements of the radial velocity. The beam crossing angle was measured both with and without the Bragg cell to an accuracy of $\pm 0.5\%$. The parallelness of the two beams before the focusing lens was also measured and found to be within 0.03 deg. The effect of this on the beam crossing location was estimated to be negligible. The distance from the beam waist to the beam crossing was also calculated and found to be smaller than the beam waist length. Therefore, it was assumed that the beams crossed at their beam waist.

To allow for precise and repeatable positioning of the probe volume within the spray, the entire optical system was mounted on an X,Y,Z tranversing table while the spray chamber remained fixed. The reported axial drop velocities were measured along the $-Z$ axis and the radial drop velocities along the $-Y$ axis (see coordinate system in Fig. 3). At each axial location, first the axis of the spray was located, based on the symmetry of the measured velocity profiles, and the radial distances were referred to it. A minimum of five measurements were made between the centerline and the half-

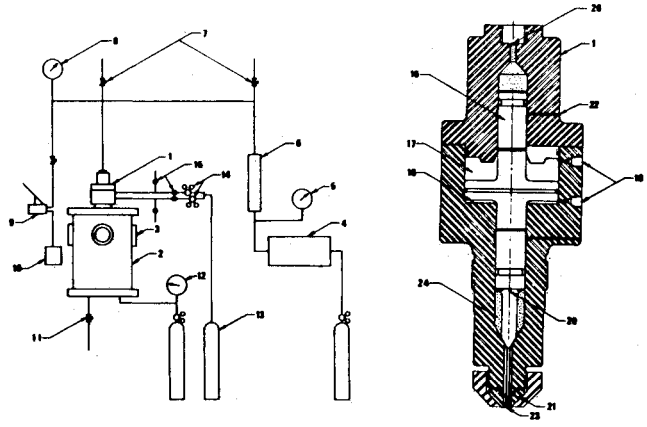

Fig. 1 Spray apparatus and details of the injection cylinder: 1) injection cylinder, 2) spray chamber, 3) window, 4) gas reservoir, 5) driver gas pressure gage, 6) liquid reservoir, 7) bleeding valves, 8) test liquid pressure gage, 9) hand pump, 10) test liquid tank, 11) drain, 12) chamber gas pressure gage, 13) nitrogen cylinder, 14) regulators, 15) solenoid valves, 16) valve unit, 17) upper control gas chamber, 18) lower control gas chamber, 19) control gas ports, 20) test liquid conduit, 21) nozzle piece, 22) leak off, 23) nozzle, 24) test liquid.

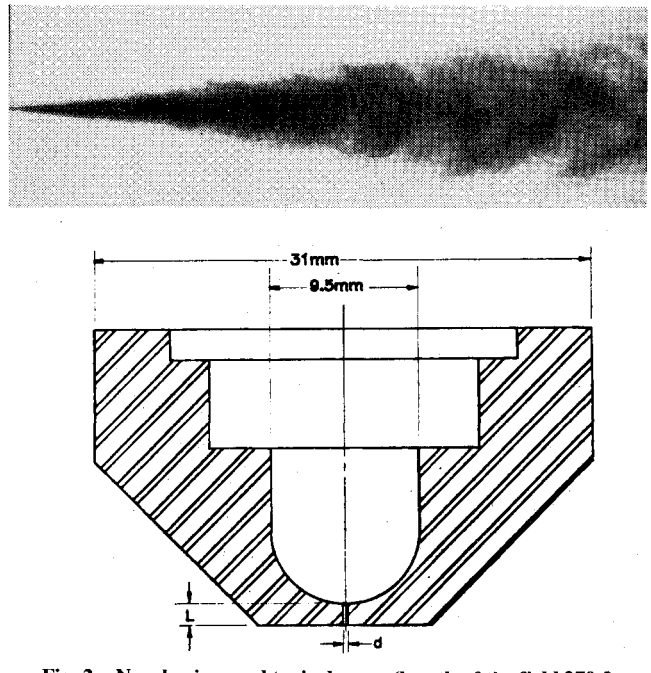

Fig. 2 Nozzle piece and typical spray (length of the field 270*d*).

Table 1 Spray conditions[a]

Series	p_g, MPa	ρ_g/ρ_ℓ	Δp, MPa	$\bar{V}_{inj}$, m/s	Nozzle, $d(\mu m)$-L/d	X/d
A	1.48	0.0256	11.0	127	127-4	600,800
B	4.24	0.0732	11.0	127	127-4	300,400,500,600
C	4.24	0.0732	26.2	194	127-4	400,500,600
D	4.24	0.0732	11.0	149	76-4	300,600,700,800
E	1.48	0.0256	11.0	125	76-1	300

[a]Liquid: n-hexane, $\rho_\ell = 665$ kg/m^3, $\mu_\ell = 3.2\times10^{4}$ N·s/m^2, $\sigma_\ell = 1.84\times10^{2}$ N/m. Gas: nitrogen. Room temperature.

Table 2 Errors in LDV measurements[10]

Source	Type	Estimated error and correction
LDV optics	Beam-crossing angle	0.5%
	Fringe spacing	No error due to refraction index
	Bragg cell	<1%
LDV electronics	Clock counting	<1% based on an intrinsic accuracy of 1 ns
	Noise	<3% with SNR = 10 and $N_{fr} = 4$
Spray	Velocity gradient	≤2% for the mean value ≤5% for fluctuation amplitude based on the maximum velocity gradient of 5(m/s)/mm
	Effect of drop size distribution	No sensible effect on velocity distribution was found for $X \geq 300d$
	Spray-to-spray variation	Negligible
	Velocity biasing	Correction applied for $RFA_{v,x} \leq 30\%$
Statistics	Axial component	≤2% for the mean value ≤3% for fluctuation amplitude based on 2000 data and 50% relative fluctuation amplitude
	Radial component	No data reported for the mean value due to large error

radius; therefore, the uncertainty in the positioning at an axial location of $300d$ is no more than $\pm 8.3\%$ of the half-radius and at axial positions further downstream the positioning error is an even smaller percentage of the half-radius.

The frequency was measured with a TSI 1990 counter processor interfaced to a Hewlett-Packard 21 MX minicomputer. The number of fringes set on the counter processor over which the frequency was measured was eight or four. Such a small number of fringes was used primarily to increase the data rate in the region of high drop number density. The use of fewer fringes also reduces the trajectory bias that can occur when a large number of fringes are used which favors drop trajectories normal to the fringe planes.[9]

The same initiation signal that operated the valve unit (item 16 in Fig. 1) was used, through a control module, to enable the counter to transmit data. The control module was also used to insert a prefixed delay between spray initiation and the start of data transmission and to program the data acquisition period for each test. The delay was necessary to allow the spray to reach a steady-state condition as determined from the time history of the liquid pressure.

All the measurements were made in steady sprays. Even though the data were taken in a 0.5-1.0 s period to prevent recirculation inside the chamber from affecting the spray, the velocity of these sprays was so high, and their size so small, that their characteristic times are much shorter than 1.0 s. The longest time would be the convection time at the farthest axial station ($800d$) for the largest of the nozzles (127 μm) and the slowest of the injection velocities (127 m/s). This time is less than 0.03 s. As previously stated, during the measurements liquid and gas pressure were constant to better than 1%. Far downstream, the 0.5-1.0 s window was long enough to collect more than 2000 data points during one injection, but going upsteam the rate of acquisition of acceptable data decreased and up to 30 injections were necessary to obtain the same total number of velocity data. For each set of measurements, the number of rejected data, based on the criterion that the data should fall within 3.5σ of the mean, was always less than 1% of the total.

Error Analysis

An extensive analysis of experimental errors was carried out. A detailed discussion is available in Ref. 10. Sources of error, their estimated magnitudes, and possible corrections are summarized in Table 2. Only the discussion of the effects of drop size distribution and velocity biasing is given here.

No direct measurement of the drop size distribution was made from which the possible correlation between drop size and velocity could be determined. However, along the axis it was found that for $X/d \geq 300$ the velocity distribution is not affected by varying the laser power or by limiting the observed range of drop sizes to which the counter processor responded (achieved by reducing the upper limit of the dc component of the Doppler signals accepted by the LDV counter processor). Figure 4 shows the effect on the mean velocity and the fluctuation amplitude at $X/d = 800$ of a variation of the amplitude limit setting on the counter processor from 100 to 2. No significant change is seen in either $\bar{V}_x$ or fluctuation amplitude whereas the data rate changed drastically, indicating a large selectivity in drop size. It was estimated that

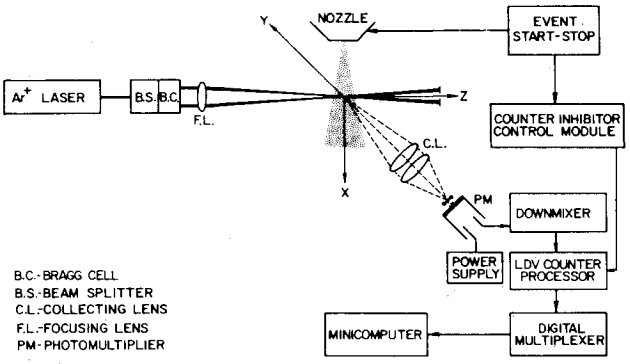

Fig. 3 LDV setup.

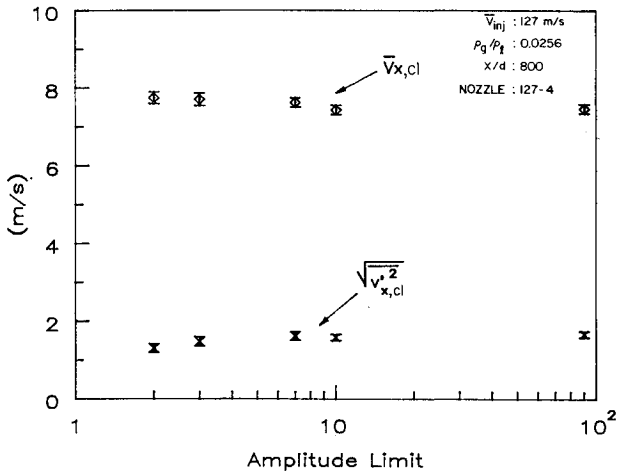

Fig. 4 Variation of mean and fluctuating components of the drop axial velocity vs amplitude limit setting of the counter processor.

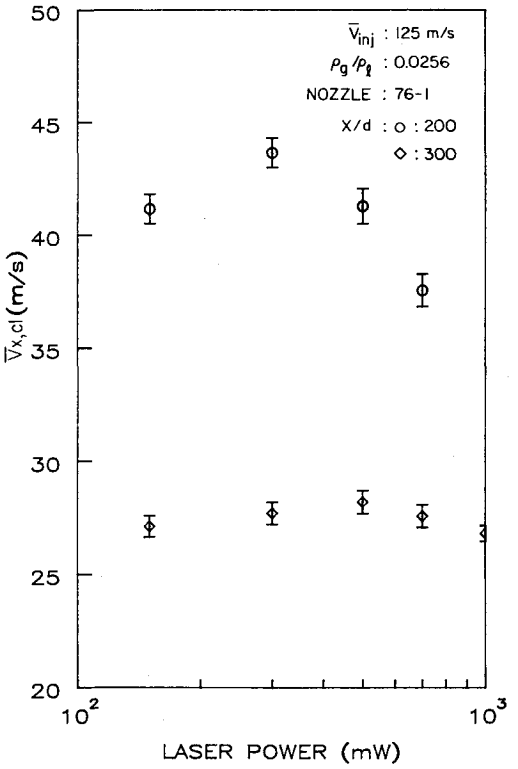

Fig. 5 Variation of mean drop axial velocity vs laser power.

at least 90% of the total number of observable drops were rejected with the lower setting.[10] However, upstream of $X/d=300$, the mean velocity begins to show sensitivity to variations of the laser power (equivalent to changing the amplitude limit setting) and at $X/d=200$ change in $\bar{V}_x$ is quite large, as shown in Fig. 5. For this reason only the measurements for $X/d\geq 300$ are reported and discussed. From the point of view of the structure of these sprays, the fact that, for $X/d\geq 300$, the drop velocity is independent of the drop size along the axis implies that drop and gas velocities there are the same; that is, the equilibrium limit has been reached. For $X/d<300$, along the spray axis it is concluded that the drop and gas velocities are different.

The major source of uncertainty in the estimates of errors was the velocity bias effects. A velocity bias error can occur in fluctuating flows since, with uniform particle concentration, more particles are sampled per unit time when the gas velocity is higher.[11,12] The magnitude of the velocity bias error depends on the local fluctuation amplitude. Buchhave[13] calculated the velocity bias errors of the mean and the fluctuating velocities for three-dimensional Gaussian isotropic turbulence, for relative turbulence intensities up to 80%, including the effects of trajectory bias but without frequency shifting and showed that the errors increase monotonically with the turbulence intensity. At 30% turbulence intensity the velocity bias errors were between 5 and 10% for the mean velocity, and between 3 and 7% for the fluctuation amplitude, depending on the ratio of the minimum number of fringe crossings required for a measurement to the maximum number of fringe crossings available.

The determination of unbiased averaged quantities from velocity biased data can be achieved only if the time each particle remains in the probe volume is known exactly.[9] A simplified one-dimensional a posteriori correction can be applied by weighting each individual measurement with a weighting factor inversely proportional to the measured velocity component.[11] This correction method can reduce the velocity bias error when the relative fluctuation amplitude is small. For example, after correction, at 30% turbulence intensity, the velocity bias errors are less than 4.3% for the mean velocity and between 2 and 5.5% for the fluctuation amplitude.[13] For our sprays the one-dimensional correction method was considered acceptable and was applied as long as the relative fluctuation of the drop velocity was less than or equal to 30%. Above 30%, the residence time can no longer be approximated by the measured velocity component and the one-dimensional correction overcorrects the mean velocity and introduces errors that can be larger in magnitude, and opposite in sign, than those of the uncorrected data. Thus, the correction does not improve the accuracy of the data and the uncorrected data may be in error by as much as 22% for the mean velocity and 10% for the fluctuation amplitude at 80% turbulence intensity if the angular dependence is minimized by frequency shifting.[13]

Besides the drop velocity distribution, the half-radius as determined from the drop axial mean velocity is also affected by the velocity bias error because at the half-radius location the fluctuation amplitude is about 45%. The half-radius was derived both from data which had been velocity bias corrected around the half-radius location (fully corrected) and from data to which no velocity bias correction had been applied around the half-radius location (partially corrected). In both cases the one-dimensional velocity bias correction was applied for relative fluctuations smaller than 30%, i.e., near the spray centerline. The two sets of half-radius results differ from each other by 10%. Buchhave[13] showed that without correction the half-radius is overestimated and with correction it is underestimated. Thus, based on half the difference of these

results the uncertainty in the half-radius due to the velocity bias error is about ±5%. But when all other sources of error are considered, the total uncertainty in the half-radius becomes ±6.6%.

The velocity bias correction is strictly valid only if the drop number density can be assumed to be uncorrelated with the local velocity and provided no other limitations on the mean sampling rate interfere and further complicate the problem. The drop concentration also must be sufficiently low so that most of the time there is only one drop in the probe volume.[11] This condition was only marginally satisfied.

In summary, the one-dimensional correction was applied on the drop velocity data as long as the relative fluctuation amplitude was less than or equal to 30%. The result was that the total maximum error of the reported mean velocity was estimated to be less than 10% up to the half-radius and increasingly larger outward where it can be as large as 40% for a relative drop velocity fluctuation amplitude of 80%. The total error of the reported fluctuation amplitudes is, in general, smaller than that of the mean velocity.

Results and Discussion

The parameters varied in the experiment are listed in Table 1. Five conditions were examined with different combinations of two gas-to-liquid density ratios, two injection pressures, and three nozzle geometries. For each condition, the axial and radial components of the drop velocity were measured by LDV at several axial and radial locations. The measurements discussed in this section were taken with 300-800 nozzle diameters from the nozzle exit (2.29-10.16 cm).

We will consider, first, average drop velocities; then, fluctuations of the drop velocities; and, finally, the implications of the measurements about the structure of these sprays. In the figures, the corresponding fluid quantities measured by Wygnanski and Fiedler[14] by hot-wire anemometry in isothermal, low Mach number (incompressible) air-into-air jets are shown for reference and comparison, but without implying that they constitute definitive measurements of incompressible jets.

Figure 6 shows that, at sufficient distance from the injector, the ratio of the centerline velocity to the injection velocity tends to depend only on $X/d\,(\rho_\ell/\rho_g)^{1/2}$. In this figure, data other than ours are from Ref. 15. According to Hinze,[18] this scaling was first proposed by Thring and Newby,[19] but was also obtained analytically by Kleinstein.[20]

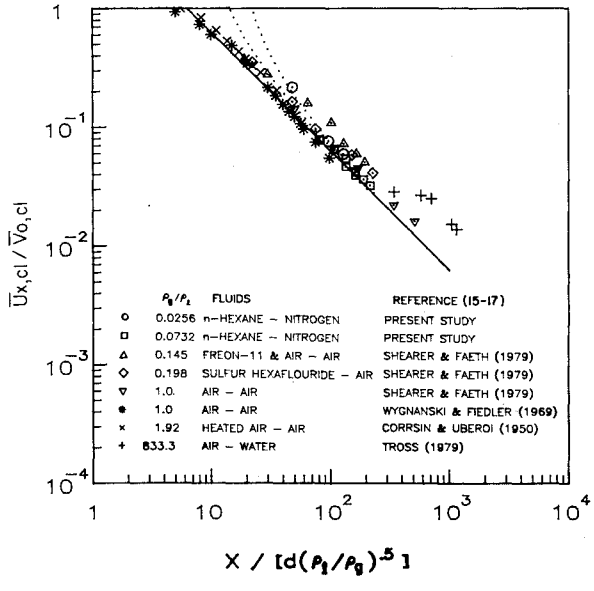

Fig. 6 Centerline velocity decay of different jets vs dimensionless axial distance.

To understand the possible reasons for the scatter of the data in Fig. 6, consider a steady injection of a fluid ℓ into a second fluid g. At sufficient distance from the injector the flow rate of the injected mass becomes negligible with respect to that of the entrained mass and the subsequent development of the jet depends on the ambient fluid entraining more ambient fluid as in "incompressible" jets. This fully developed incompressible jet limit must eventually be reached independently of the nature of the fluids and of the structure of the development region. Then, neglecting viscous stresses and pressure gradients, conservation of axial momentum gives

$$C_\ell \rho_\ell \bar{V}^2_{0,cl} d^2/4 = C_g \rho_g \bar{U}^2_{x,cl} r^2_{0.5,g} \tag{1}$$

$$\frac{\bar{U}_{x,cl}}{\bar{V}_{0,cl}} = \left(\frac{C_\ell}{4C_g C^2}\right)^{1/2} \frac{d(\rho_\ell/\rho_g)^{1/2}}{X - X_0} \tag{2}$$

where C_g relates the self-preserving distributions of the mean axial velocity and velocity fluctuations to the mean centerline velocity and is equal[14,16,23] to 0.846±2.9%; $C = 0.0868 \pm 7.9\%$ relates the half-radius to the distance from X_0, the virtual origin[14,21-23]; and C_ℓ relates the injection momentum to the injection centerline velocity. For uniform injection velocity profile $C_\ell = 1$ and the coefficient of Eq. (2) is 6.3±9% (Capp

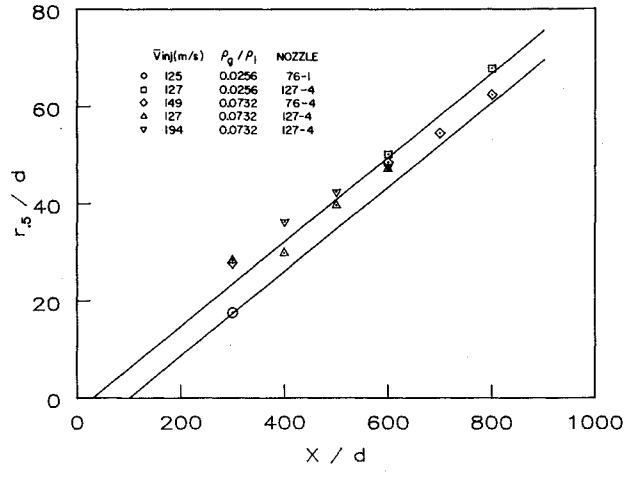

Fig. 7 Dimensionless half-radius of the drop axial velocity vs dimensionless axial distance.

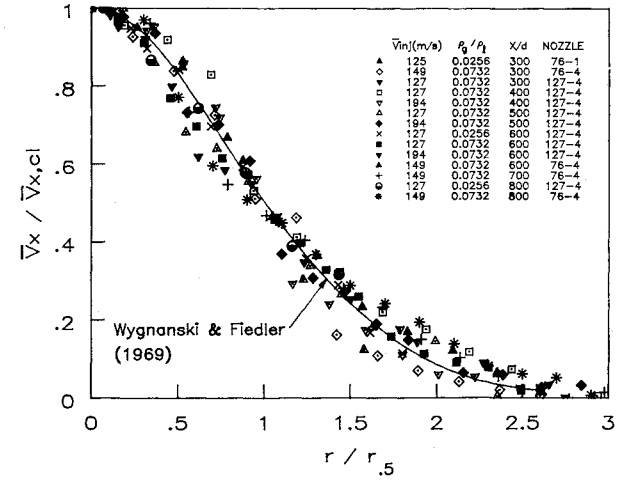

Fig. 8 Self-similar profile of the dimensionless mean drop axial velocity.

and George,[23] for example, give 5.8). In Fig. 6 the continuous line corresponds to $X_0=0$ whereas the two dotted lines correspond to $(X_0/d)/(\rho_\ell/\rho_g)^{1/2}=30/(13.7)^{1/2}$ and $100/(39.1)^{1/2}=8.12$ and 16.0, respectively. The X_0 values of 30 and 100 will be explained later. The three lines show that, at sufficient distance from the injector, the structure and length of the development region become immaterial.

Often there is uncertainty about the value of C_ℓ for different experiments because the injection momentum generally is not measured and because different authors may use velocities other than the centerline velocity as reference injection velocity. As previously stated, we did not measure the injection velocity profile. We measured the mass mean injection velocity, $\bar{V}_{\text{inj}}$, and estimated that the injection momentum was equal to $C_\ell\rho_\ell\bar{V}_{\text{inj}}^2\pi d^2/4$ with $C_\ell=1\pm10\%$. Thus, using $\bar{V}_{\text{inj}}$ for $V_{0,\text{cl}}$ in Fig. 6 far from the injector our data must fall on the continuous line. For data other than ours we used the injection velocity given by the various authors. We believe that the main reason for the scatter of the data at large values of $X/d\,(\rho_\ell/\rho_g)^{1/2}$ is the uncertainty about the injection momentum, i.e., about the value of C_ℓ.

Another factor could be that the fully developed local equilibrium condition was not reached by all the jets of the figure, as suggested by Shearer and Faeth.[15] For $X/d\geq300$, earlier it was shown that drop and gas velocity tend to be the same along the axis and, presently, it will be shown that mean and fluctuating components of the drop velocity have reached self-preserving profiles. Thus, the conditions for convergence to the solid line of Fig. 6 are met and our data tend to fall on it.

Finally, accurate measurements in these jets continue to be difficult and experimental errors may be present. For example, the data of Wygnanski and Fiedler are seen to tend to a different slope in Fig. 6, but Capp and George[23] report that their faster decay may be due to wall effects.

Equation (2) can now be used to determine somewhat more precisely the virtual origin. If $\bar{V}_{\text{inj}}/\bar{U}_{x,\text{cl}}$ is plotted vs X in linear scales, our far-field data must converge on straight lines of known slope, corresponding to the continuous line of Fig. 6. By extrapolating backward, the intersections of these lines determine the virtual origins. We found $X_0=30d$ for $\rho_\ell/\rho_g=13.7$ and $X_0=100d$ for $\rho_\ell/\rho_g=39.1$, the other variables having no clear effect on X_0 within the accuracy of our data. Obviously, the convergence to fully developed jets occurs further downstream in our sprays than in incompressible jets ($\rho_\ell/\rho_g=1.0$) for which the reported X_0/d is always smaller than 10. Having the virtual origins, the value of C was determined by curve fitting the measured half-radius data (Fig. 7), and found to agree with the value obtained from incompressible jet data.

Another implication of Eq. (2) is that the tip penetration rate of sprays for constant pressure injection into a stationary unconfined gas can be estimated using the injection momentum and the nozzle diameter, and without detailed knowledge of their structure. The estimate is only rough near the injector but becomes accurate far from it. This is because under such conditions the velocity of the tip of a transient spray is close to 70% of the local steady-state centerline velocity.[24,25]

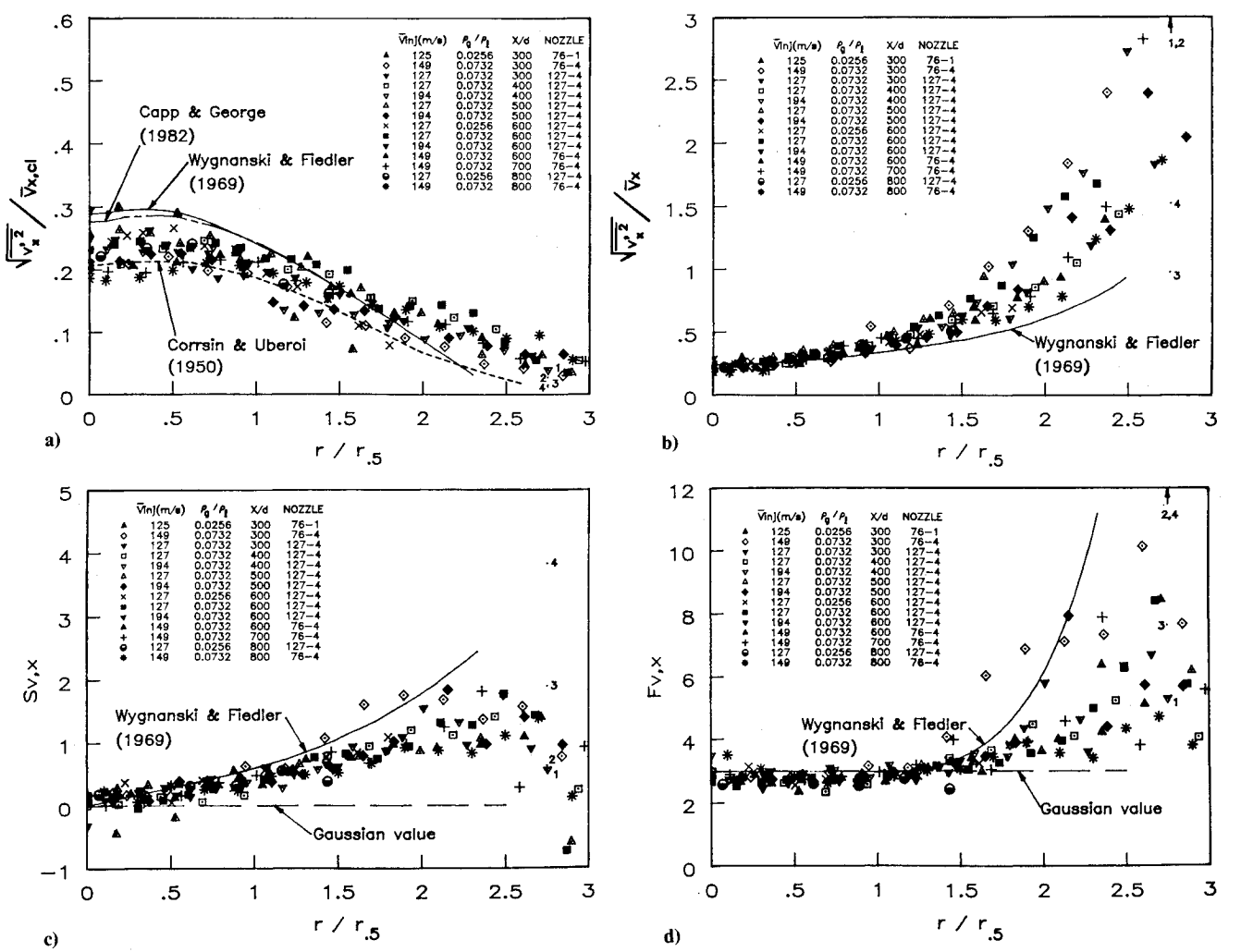

Fig. 9 Self-similar profiles of the dimensionless fluctuation of the drop axial velocity: a) dimensionless fluctuation amplitude, b) relative fluctuation amplitude, c) skewness, and d) flatness.

So far we have considered only the mean centerline velocity and the half-radius. Figure 8 shows that for $X/d \geq 300$ the parallel between the mean axial drop velocity in our sprays and the mean axial fluid velocity of incompressible jets extends to all axial and radial locations and all conditions.

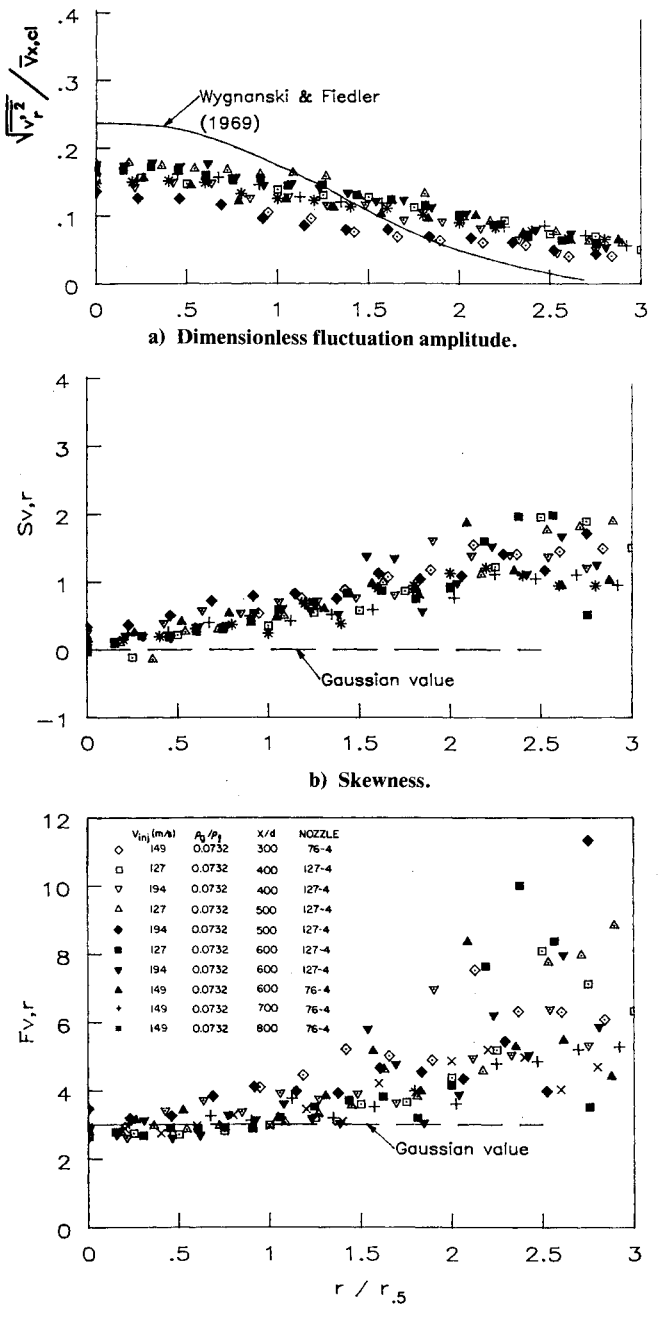

a) Dimensionless fluctuation amplitude.

b) Skewness.

c) Flatness.

Fig. 10 Self-similar profiles of the dimensionless fluctuation of the drop radial velocity.

The parallel extends also to the fluctuating components of drop and fluid velocities but with increasing uncertainty. At each axial and radial location the measured axial and radial components of the drop velocity show a distribution of values. The standard deviation and skewness and flatness of these distributions are shown in Figs. 9 and 10. It is seen that near the axis, the amplitude of the velocity fluctuation of the drops falls into the lower part of the range of incompressible jets and appears to be larger at the edge. Near the axis the distribution of the drop velocity is also Gaussian, as indicated by the skewness and flatness. At the edge of the sprays the shapes of the spray drop and incompressible jet velocity distributions appear to differ. Those of the drops tend to remain more Gaussian.

The effects of corrections and differences between experimental techniques on the disparity between the drop velocities at the edge of our sprays and the fluid velocity at the edge of incompressible jets were evaluated for the case $\Delta p = 26.2$ MPa, $p_g = 4.24$ MPa, nozzle 127-4, $X/d = 400$, and $r = 2.75 r_{0.5}$. Results are shown in Fig. 9 (numbered 1-4 at $r/r_{0.5} = 2.75$) and Table 3. The measured drop velocity distribution is nearly Gaussian without the one-dimensional correction (results 1 in the skewness and flatness graphs) but if the one-dimensional correction is applied it becomes much narrower (test 2 in Table 3) and its parameters move closer to the incompressible jet values (results 2 in flatness graph). Since the real quantities are most likely between the corrected and the uncorrected ones, there is a tendency toward better agreement.

The influence of the measuring technique appears to be even stronger and to tend to further close the gap between our results and those of the incompressible jet. It is recalled that most of the incompressible jet data, including those of Wygnanski and Fiedler, were taken with hot-wire anemometry. We can approximate the spray data that would have been obtained by hot-wire anemometry by disregarding the direction of the drop velocity as determined by the Bragg cell. The spray data thus obtained would move closer to the corresponding incompressible jet data as shown by results 3 and 4 in Table 3 and Fig. 9. Intermittency can also contribute to explaining the differences. Our drops come to the edge of the spray primarily with the gas from the core and reflect the fluctuations of this gas. Fluctuations that are averaged also over the potential fluid would be of smaller amplitude.

Thus, it is likely that the difference between our drop velocity at the edge of our sprays and the corresponding fluid velocity at the edge of incompressible jets is less than shown in Fig. 9. However, correct values cannot be established at this time.

In summary, indications are that for $X/d \geq 300$, drops and gas are nearly in equilibrium. As a further elaboration of the question of equilibrium, estimates of the characteristic relaxation times of drop velocity[26] and gas turbulence[27] were considered.[10] It was concluded that at $X = 300d$ the condition for local equilibrium should be met at least by the more numerous, smaller drops. Downstream of $X = 300d$, the drop relaxation time does not increase appreciably, because collisions and coalescence are no longer numerous at low liquid-volume fractions,[28] whereas the turbulent eddy time continues to increase as X^2. Thus, a station is reached at

Table 3 Effects of the Bragg cell and the one-dimensional correction on the drop velocity distribution

Test	Bragg cell	Correction	$\bar{V}_x$, m/s	$\sqrt{V_x'^2}$, m/s	$S_{v,x}$	$F_{v,x}$
1	Yes	No	0.024	0.503	0.57	5.32
2	Yes	1-D	0.003	0.198	0.63	18.44
3	No	No	0.360	0.351	1.89	7.63
4	No	1-D	0.109	0.166	3.82	25.16

which most of the drops are in equilibrium with most of the eddies.

Finally, it is recalled that for $X<300d$ all indications are that local equilibrium is not present. This lack of equilibrium near the injector and a successive but selective equilibration process downstream are in general agreement with those described by Faeth.[29]

Summary and Conclusions

Axial and radial components of the drop velocity were measured by LDV at numerous radial and axial locations ($300 \leq X/d \leq 800$) within diesel-type n-hexane sprays but at room temperature, under steady injection pressure, and into initially quiescent nitrogen. Five configurations were employed that differed in gas-to-liquid density ratio (0.0256, 0.0732), injection velocity (127, 149, and 194 m/s), and nozzle geometry (straight cylindrical holes with sharp inlet and outlet, diameters of 76 and 127 μm, and length-to-diameter ratio of 4 and 1). The LDV system was made up of an argon-ion laser, TSI dual beam LDV optics with a Bragg cell, 90-deg scatter collection optics, counter processor, and minicomputer.

In the error analysis we considered errors related to the LDV optics, LDV electronics, velocity gradient broadening, drop size distribution, drop number density, probe volume position, finite sample size, and velocity bias. The magnitude of the velocity bias error was particularly difficult to estimate but it was concluded that for the reported data the total error is less than 10% from the centerline to the half-radius and progressively greater and more difficult to evaluate beyond the half-radius. Significant uncertainties about the magnitude of errors at the outer edge of jets with either LDV or hot-wire anemometry suggest that this region is still poorly characterized even for incompressible jets.

It was found that at sufficient distance from the nozzle so much gas has been entrained that the subsequent structure of the spray is dominated by the entrained gas and that the fully developed incompressible jet structure and the equilibrium limit are reached. This condition is being approached 300 nozzle diameters from the nozzle as shown by all the measured drop velocity parameters: jet half-radius, centerline velocity decay, axial mean velocity distribution, axial and radial velocity fluctuation distributions, and independence of drop velocity on drop size. However, the condition is not verified at distances smaller than 300 nozzle diameters.

For engine applications, the distance up to 300 nozzle diameters, i.e., the first 3-12 cm, is the one of prime interest. If it is true that vaporization should speed up the achievement of the fully developed state, it is also true that neither the ambient gas nor the injection pressure are steady during fuel injection and, therefore, accurate computations of engine sprays are likely to require knowledge of the non-equilibrium developing region.

On the other hand, under steady conditions it is possible to estimate the steady-state centerline velocity and the tip penetration rate for a broad range of density ratios using only the injection momentum and the nozzle diameter. The estimate becomes accurate far from the injector.

Acknowledgments

Support for this work was provided by the Army Research Office (DAAG29-81-K-0135), the Department of Energy (DE-AC-04-81AL16338), General Motors, and Cummins Engine. We are grateful to the anonymous reviewers of this article whose unusually precise comments helped us improve its clarity.

References

[1] Giffen, E. and Muraszew, A., *The Atomization of Liquid Fuels,* John Wiley and Sons, New York, 1953.

[2] Dombrowski, N. and Mundy, G., "Spray Drying," *Biochemical and Biological Engineering Science,* Vol. 22, Academic Press, New York, 1968.

[3] Taylor, C. F., *The Internal Combustion Engine in Theory and Practice,* MIT Press, Cambridge, Mass., 1966.

[4] Obert, E. F., *Internal Combustion Engines,* International Textbook Co., Scranton, Pa., 1973.

[5] Reitz, R. D. and Bracco, F. V., "Mechanism of Atomization of a Liquid Jet," *Physics of Fluids,* Vol. 25, Oct. 1982, pp. 1730-1742.

[6] Wu, K.-J., Su, C.-C., Steinberger, R.L., Santavicca, D. A., and Bracco, F. V., "Measurements of the Spray Angle of Atomizing Jets," *Journal of Fluids Engineering,* Vol. 105, Dec. 1983, pp. 406-415.

[7] Hiroyasu, H., Shimizu, M., and Arai, M., "The Breakup of High Speed Jet in a High Pressure Gaseous Atmosphere," ICLASS-82, Madison, Wis. 1982.

[8] Yule, A. J., Ah Seng, C., Felton, P. G., Ungut, A., and Chigier, N. A., "Sprays, Drops, Dusts, Particles: A Study of Vaporizing Fuel Sprays by Laser Techniques," *Combustion and Flame,* Vol. 44, Jan. 1982, pp. 71-84.

[9] Buchhave, R., George, W. K. Jr., and Lumley, J. L., "The Measurement of Turbulence with the Laser-Doppler Anemometer," *Annual Review of Fluid Mechanics,* 1979, pp. 443-503.

[10] Wu, K.-J., "Atomizing Round Jets," Ph.D. Thesis 1612-T, Dept. of Mechanical and Aerospace Engineering, Princeton Univ., N.J., Aug. 1983.

[11] McLaughlin, D. K. and Tiederman, W. G., "Biasing Correction for Individual Realization of Laser Anemometer Measurements in Turbulent Flows," *Physics of Fluids,* Vol. 16, No. 12, 1973, pp. 2082-2088.

[12] Dimotakis, P. E., "Single Scattering Particle Laser-Doppler Measurements of Turbulence," AGARD CP-193, Saint-Louis, France, 1976.

[13] Buchhave, P., "Biasing Errors in Individual Particle Measurements with the LDA-Counter Signal Processor," *Proceedings of the LDA Symposium,* Copenhagen, 1975, pp. 258-278.

[14] Wygnanski, I. and Fiedler, H., "Some Measurements in the Self-Preserving Jets," *Journal of Fluid Mechanics,* Vol. 38, Sept. 1969, pp. 577-612.

[15] Shearer, A. J. and Faeth, G. M., "Evaluation of a Locally Homogeneous Model of Spray Evaporation," NASA CR-3198, 1979.

[16] Corrsin, S. and Uberoi, M. S., "Further Experiments on the Flow and Heat Transfer in a Heated Turbulent Air Jet," NACA TR998, 1950.

[17] Tross, S. R., "Characteristics of a Submerged Two-Phase Free Jet," M.S. Thesis, The Pennsylvania State Univ., University Park, Pa. 1974.

[18] Hinze, J. O., *Turbulence,* second ed., McGraw-Hill, New York, 1975.

[19] Thring, H. W. and Newby, M. P., "Combustion Length of Enclosed Turbulent Jet Flames," *4th Symposium on Combustion,* Williams and Wilkins Co., Baltimore, Md., 1953, pp. 789-796.

[20] Kleinstein, G., "Mixing in Turbulent Axially Symmetric Free Jets," *Journal of Spacecraft and Rockets,* Vol. 1, July 1964, pp. 403-408.

[21] Hoesel, W. and Rodi, W., "New Biasing Elimination Method for Laser-Doppler Velocimeter Counter Processing," *Review of Scientific Instruments,* Vol. 48, July 1977, pp. 910-919.

[22] Schlichting, H., *Boundary Layer Theory,* seventh ed., McGraw-Hill, New York, 1979.

[23] Capp, S. P. and George, W. K. Jr., "Measurements in an Axisymmetric Jet Using a Two-Color LDA and Burst Processing," International Symposium on Applied LDA to Fluid Mechanics, Lisbon, Portugal, 1982.

[24] Kuo, T.-W. and Bracco, F. V., "On the Scaling of Transient Laminar, Turbulent, and Spray Jets," SAE Paper 820038, Warrendale, Pa., Feb. 1982.

[25] Whitehouse, N. D. and Sareen, B. K., "Prediction of Heat Release in a Quiescent Chamber Diesel Engine Allowing for Fuel/Air Mixing," SAE Paper 740084, Warrendale, Pa., Nov. 1974.

[26] Owen, P. R., "Pneumatic Transport," *Journal of Fluid Mechanics,* Vol. 39, Nov. 1969, pp. 407-432.

[27] Launder, B. E. and Spalding, D. B., *Lectures in Mathematical Models of Turbulence,* Academic Press, London, 1972.

[28] O'Rourke, P. J. and Bracco, F. V., "Modeling of Drop Interactions in Thick Sprays and Comparison with Experiments," *Institute of Mechanical Engineers,* Pub. ISBN 0 85298 4693, Nov. 1980, pp. 101-116.

[29] Faeth, G. M., "Evaporation and Combustion of Sprays," *Progress in Energy and Combustion Science,* Vol. 9, 1983, pp. 1-76.